

Twins: Revisiting the Design of Spatial Attention in Vision Transformers

Xiangxiang Chu¹, Zhi Tian², Yuqing Wang¹, Bo Zhang¹,
 Haibing Ren¹, Xiaolin Wei¹, Huaxia Xia¹, Chunhua Shen^{2*}

¹ Meituan Inc. ² The University of Adelaide, Australia

¹ {chuxiangxiang, wangyuqing06, zhangbo97, renhaibing, weixiaolin02, xiahuaxia}@meituan.com
² zhi.tian@outlook.com, chunhua@me.com

Abstract

Very recently, a variety of vision transformer architectures for dense prediction tasks have been proposed and they show that the design of spatial attention is critical to their success in these tasks. In this work, we revisit the design of the spatial attention and demonstrate that a carefully-devised yet simple spatial attention mechanism performs favourably against the state-of-the-art schemes. As a result, we propose two vision transformer architectures, namely, Twins-PCPVT and Twins-SVT. Our proposed architectures are highly-efficient and easy to implement, only involving matrix multiplications that are highly optimized in modern deep learning frameworks. More importantly, the proposed architectures achieve excellent performance on a wide range of visual tasks including image-level classification as well as dense detection and segmentation. The simplicity and strong performance suggest that our proposed architectures may serve as stronger backbones for many vision tasks. Our code will be released soon at <https://github.com/Meituan-AutoML/Twins>.

1 Introduction

Recently, Vision Transformers [1–3] have received increasingly research interest. Compared to the widely-used convolutional neural networks (CNNs) in visual perception, Vision Transformers enjoy great flexibility in modeling long-range dependencies in vision tasks, introduce less inductive bias, and can naturally process multi-modality input data including image, video, text, speech signal and point cloud. Thus, they have been considered to be a strong alternative to CNNs. It is expected that vision transformers are likely to replace CNNs and serve as the most basic component in the next-generation visual perception systems.

One of the prominent problems when applying transformers to vision tasks is the heavy computational complexity incurred by the spatial self-attention operation in transformers, which grows quadratically in the number of pixels of the input image. A workaround is the *locally-grouped self-attention* (or self-attention in non-overlapped windows as in the recent Swin Transformer [4]), where the input is spatially grouped into non-overlapped windows and the standard self-attention is computed only within each sub-window. Although it can significantly reduce the complexity, it lacks the connections between different windows and thus results in a limited receptive field. As pointed out by many previous works [5–7], a sufficiently large receptive field is crucial to the performance, particularly for dense prediction tasks such as image segmentation and object detection. Swin [4] proposes a shifted window operation to tackle the issue, where the boundaries of these local windows are gradually moved as the network proceeds. Despite of being effective, the shifted windows may have uneven

*Corresponding author.

sizes. The uneven windows also result in difficulties when implemented using modern deep learning frameworks, which prefer the windows of equal sizes. Another solution is proposed in PVT [8]. Unlike the standard self-attention operation, where each query computes the attention weights with all the input tokens, in PVT, each query only computes the attention with a sub-sampled version of the input tokens. In theory, its computational complexity is still quadratic, but it is already manageable in practice.

From a unified perspective, the key in the aforementioned vision transformers is how the spatial attention is designed. Thus, in this work, we revisit the design of the spatial attention in vision transformers. Our first finding is that the global sub-sampled attention in PVT is highly effective, and with the correct positional encodings [9], its performance can be on par or even better than all state-of-the-art vision transformers (*e.g.*, Swin). This results in our first proposed architecture, termed *Twins-PCPVT*. On top of that, we further propose a *carefully-designed yet simple spatial attention* mechanism to replace the less efficient global sub-sampled attention in PVT. Our attention mechanism is inspired by the widely-used separable depthwise convolutions and thus we name it *spatially separable self-attention* (SSSA). Our proposed SSSA is composed of two types of attention operations—(i) *locally-grouped self-attention* (LSA), and (ii) *global sub-sampled attention* (GSA), where LSA captures the fine-grained and short-distance information and GSA deals with the long-distance and global information. Both attention operations are *efficient and easy-to-implement* with matrix multiplications in a few lines of code. This leads to the second proposed vision transformer architecture, termed *Twins-SVT*.

We benchmark our proposed architectures on a number of visual tasks, ranging from image-level classification to pixel-level semantic/instance segmentation and object detection. Extensive experiments show that both of our proposed architectures perform favourably against other state-of-the-art vision transformers with similar or even reduced computational complexity.

2 Related Work

Convolutional neural networks. Characterized by local connectivity, weight sharing, shift-invariance and pooling, CNNs have been the *de facto* model for computer vision tasks. The top-performing models [10–19] in image classification also serve as the strong backbones for downstream detection and segmentation tasks.

Vision Transformers. Transformers were firstly proposed by [20] for machine translation tasks, and since then they have become the state-of-the-art models for NLP tasks, overtaking the sequence-to-sequence approach built on LSTM. Its core component is multi-head self-attention which models the relationship between input tokens and shows great flexibility.

In 2020, transformers were introduced to computer vision for image and video processing [1–3, 9, 21–23, 23–38]. In the image classification task, ViT [1] and DeiT [2] divide the images into patch embedding sequences and feed them into the standard transformers. Although vision transformers have been proved compelling in image classification compared with CNNs, a challenge remains when it is applied to dense prediction tasks such as object detection and segmentation. These tasks often require feature pyramids for better processing objects of different scales, and take as inputs the high-resolution images, which significantly increase the computational complexity of the self-attention operations.

Recently, Pyramid Vision Transformer (PVT) [8] is proposed and can output the feature pyramid [39] as in CNNs. PVT has demonstrated good performance in a number of dense prediction tasks. The recent Swin Transformer [4] introduces non-overlapping window partitions and restricts self-attention within each local window, resulting in linear computational complexity in the number of input tokens. To interchange information among different local areas, its window partitions are particularly designed to shift between two adjacent self-attention layers.

Grouped and Separable Convolutions. Grouped convolutions are originally proposed in AlexNet [10] for distributed computing. They were proved both efficient and effective in speeding up the networks. As an extreme case, depthwise convolutions [14, 40] use the number of groups that is equal to the input or output channels, which is followed by point-wise convolutions to aggregate the information across different channels. Here, the proposed spatially separable self-attention shares some similarities with them.

Positional Encodings. Most vision transformers use absolute/relative positional encodings, depending on downstream tasks, which are based on sinusoidal functions [20] or learnable [1, 2]. In CPVT [9], the authors propose the conditional positional encodings, which are dynamically conditioned on the inputs and show better performance than the absolute and relative ones.

3 Our Method: Twins

We present two simple yet powerful spatial designs for vision transformers. The first method is built upon PVT [8] and CPVT [9], which only uses the global attention. The architecture is thus termed Twins-PCPVT. The second one, termed Twins-SVT, is based on the proposed SSSA which interleaves local and global attention.

3.1 Twins-PCPVT

PVT [8] introduces the pyramid multi-stage design to better tackle dense prediction tasks such as object detection and semantic segmentation. It inherits the learnable positional encoding designed in ViT [1] and DeiT [2]. All layers utilize the global attention mechanism and rely on spatial reduction to cut down the computation cost of processing the whole sequence. It is surprising to see that the recently-proposed Swin transformer [4], which is based on shifted local windows, can perform considerably better than PVT, even on dense prediction tasks where a sufficiently large receptive field is even more crucial to good performance.

In this work, we surprisingly found that the less favored performance of PVT is simply due to the *absolute positional encodings* employed in PVT [8]. There is a significant difference between classification and dense prediction tasks, particularly in the training stage. The classification task only deals with fixed-size images while the dense prediction tasks take as inputs varying-size images. As shown in CPVT [9], the predefined absolute positional encoding encounter difficulties in processing the inputs with varying sizes. Moreover, this positional encoding also breaks the translation-invariance. On the contrary, Swin transformer makes use of the relative positional encodings, which bypass the above issues. Here, we demonstrate that this is the root cause why Swin outperforms PVT, and we show that if the appropriate positional encodings are used, PVT can actually achieve on par or even better performance than the Swin transformer.

Here, we use the conditional position encoding (CPE) proposed in CPVT [9] to replace the absolute PE in PVT. CPE is conditioned on the inputs and can naturally bypass the above issues of the absolute encoding. The position encoding generator (PEG) [9], which generates the CPE, is placed after the first encoder block of each stage. We use the simplest form of PEG, *i.e.*, a 2D depth-wise convolution without batch normalization. For image-level classification, following CPVT, we remove the class token and use global average pooling (GAP) at the end of the stage [9]. For other vision tasks, we follow the design of PVT. Twins-PCPVT inherits the advantages of both PVT and CPVT, which makes it easy to implement efficiently. Our extensive experimental results show that this simple design can match the performance of the recent state-of-the-art Swin transformer. We have also attempted to replace the relative positional encodings with CPE in Swin, which however does not result in noticeable performance gains, as shown in our experiments. We conjecture that this may be due to the use of shifted windows in Swin.

Architecture settings We report the details of the settings of Twins-PCPVT in Table 1, which are similar to PVT [8]. Therefore, Twins-PCPVT has similar FLOPs and number of parameters compared to [8].

3.2 Twins-SVT

Vision transformers suffer severely from the heavy computational complexity in dense prediction tasks due to high resolution inputs. Given an input of $H \times W$ resolution, the complexity of self-attention with dimension d is $\mathcal{O}(H^2W^2d)$. Here, we propose the spatially separable self-attention (SSSA) to alleviate this challenge. SSSA is composed of locally-grouped self-attention (LSA) and global sub-sampled attention (GSA).

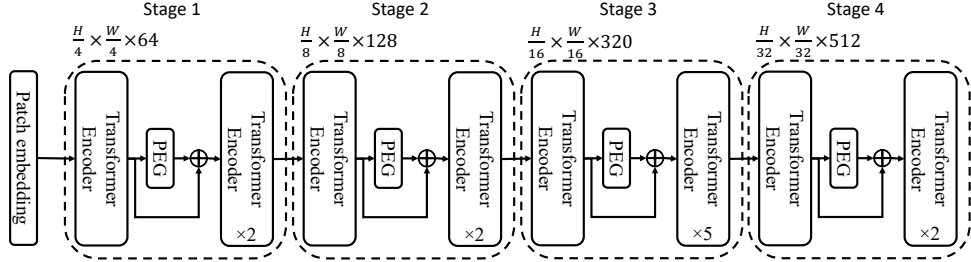


Figure 1 – Architecture of Twins-PCPVT-S.

Table 1 – Configuration details of Twins-PCPVT.

	Output Size	Layer Name	Twins-PCPVT-S	Twins-PCPVT-B	Twins-PCPVT-L
Stage 1	$\frac{H}{4} \times \frac{W}{4}$	Patch Embedding	$P_1 = 4; C_1 = 64$		
		Transformer Encoder with PEG	$R_1 = 8$ $N_1 = 1$ $E_1 = 8$	$R_1 = 8$ $N_1 = 1$ $E_1 = 8$	$R_1 = 8$ $N_1 = 1$ $E_1 = 8$
Stage 2	$\frac{H}{8} \times \frac{W}{8}$	Patch Embedding	$P_2 = 2; C_2 = 128$		
		Transformer Encoder with PEG	$R_2 = 4$ $N_2 = 2$ $E_2 = 8$	$R_2 = 4$ $N_2 = 2$ $E_2 = 8$	$R_2 = 4$ $N_2 = 2$ $E_2 = 8$
Stage 3	$\frac{H}{16} \times \frac{W}{16}$	Patch Embedding	$P_3 = 2; C_3 = 320$		
		Transformer Encoder with PEG	$R_3 = 2$ $N_3 = 5$ $E_3 = 4$	$R_3 = 2$ $N_3 = 5$ $E_3 = 4$	$R_3 = 2$ $N_3 = 5$ $E_3 = 4$
Stage 4	$\frac{H}{32} \times \frac{W}{32}$	Patch Embedding	$P_4 = 2; C_4 = 512$		
		Transformer Encoder with PEG	$R_4 = 1$ $N_4 = 8$ $E_4 = 4$	$R_4 = 1$ $N_4 = 8$ $E_4 = 4$	$R_4 = 1$ $N_4 = 8$ $E_4 = 4$

Locally-grouped self-attention (LSA). Motivated by the separable convolution design for efficient inference, we first equally divide the 2D feature maps into sub-windows, making self-attention communications only happen within each sub-window. To be specific, the feature maps are divided into $m \times n$ sub-windows. Without loss of generality, we assume $H \% m = 0$ and $W \% n = 0$. Each group contains $\frac{HW}{mn}$ elements with computation cost $\mathcal{O}(\frac{H^2W^2}{m^2n^2}d)$. The total cost is $\mathcal{O}(\frac{H^2W^2}{mn}d)$. If we use $k_1 = \frac{H}{m}$, $k_2 = \frac{W}{n}$, the cost can be computed as $\mathcal{O}(k_1k_2HWd)$, which is significantly more efficient when $k_1 \ll H$ and $k_2 \ll W$ and grows linearly with HW if k_1 and k_2 are fixed.

Although the locally-grouped self-attention mechanism is computation friendly, the image is divided into non-overlapping sub-windows. Thus, we need a mechanism to communicate between different sub-windows, as in Swin. Otherwise, the information would be always limited to be processed locally and the receptive field is thus $k_1 \times k_2$, which significantly degrades the performance as shown in our experiments. This resembles the fact that we cannot replace all standard convolutions by depth-wise convolutions in CNNs.

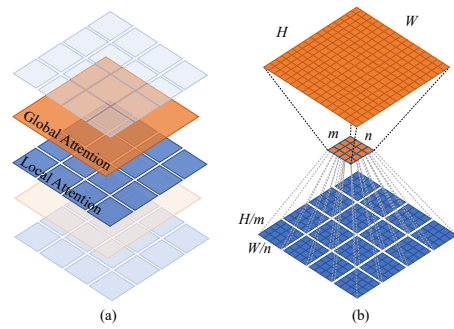


Figure 2 – (a) Twins-SVT interleaves locally-grouped attention (LSA) and global sub-sampled attention (GSA). (b) Schematic view of the locally-grouped attention (LSA) and global sub-sampled attention (GSA).

Global sub-sampled attention (GSA). A simple solution is to add extra standard global self-attention layers after each local attention block, so as to enable cross-group information exchange. Our experiments in the sequel prove the effectiveness of this design. However, this approach would come with the computation complexity of $\mathcal{O}(H^2W^2d)$.

If we use a single representative to summarize the key information within each sub-window and the representative is used to communicate with other sub-windows (serving as the key in self-attention), the global attention cost would be dramatically reduced to $\mathcal{O}(mnHWd) = \mathcal{O}(\frac{H^2W^2d}{k_1k_2})$. This is essentially equivalent to using the sub-sampled feature maps as the key in self-attention, and thus we term it global sub-sampled attention (GSA). If we alternatively use the locally-grouped self-attention and global sub-sampled attention like separable convolutions (depth-wise + point-wise). The total computation cost is $\mathcal{O}(\frac{H^2W^2d}{k_1k_2} + k_1k_2HWd)$. We have $\frac{H^2W^2d}{k_1k_2} + k_1k_2HWd \geq 2HWd\sqrt{HW}$. The minimum is obtained when $k_1 \cdot k_2 = \sqrt{HW}$. We know that $H = W = 224$ is popular in classification. Without loss of generality, we use square group, *i.e.*, $k_1 = k_2$. Therefore, $k_1 = k_2 = 15$ is close to the global minimum for $H = W = 224$. However, our network is designed to include several stages. Stage 1 has feature maps of 56×56 , the minimum is obtained when $k_1 = k_2 = \sqrt{56} \approx 7$. Theoretically, we can calibrate optimal k_1 and k_2 for different stages. For simplicity, we use $k_1 = k_2 = 7$ everywhere.

As for the sub-sampling function, we investigate several options including average pooling, depth-wise strided convolutions, and regular strided convolutions. Empirical results show that regular strided convolutions perform best here. Formally, the separable like transformer block can be written as

$$\begin{aligned} \hat{\mathbf{z}}_{ij}^l &= \text{LSA}(\text{LayerNorm}(\mathbf{z}_{ij}^{l-1})) + \mathbf{z}_{ij}^{l-1}, \\ \mathbf{z}_{ij}^l &= \text{FFN}(\text{LayerNorm}(\hat{\mathbf{z}}_{ij}^l)) + \hat{\mathbf{z}}_{ij}^l, \\ \hat{\mathbf{z}}^{l+1} &= \text{GSA}(\text{LayerNorm}(\mathbf{z}^l)) + \mathbf{z}^l, \\ \mathbf{z}^{l+1} &= \text{FFN}(\text{LayerNorm}(\hat{\mathbf{z}}^{l+1})) + \hat{\mathbf{z}}^{l+1}, \\ i &\in \{1, 2, \dots, m\}, j \in \{1, 2, \dots, n\} \end{aligned} \tag{1}$$

where LSA means locally-grouped self-attention within a sub-window; GSA is the global sub-sampled attention by interacting with the representative keys from all sub-windows and $\hat{\mathbf{z}}_{ij} \in \mathcal{R}^{k_1 \times k_2 \times C}$. Both LSA and GSA have multiple heads as in the standard self-attention. The PyTorch code of locally grouped attention is given in Algorithm 1.

Again, we use the PEG of CPVT [9] to encode position encodings and process variable-length inputs on the fly. It is inserted after the first block in each stage.

Model variants The detailed config for models is shown in Table 2. We try to use the similar settings as in Swin [4] to make sure that the good performance is from the new design paradigm except for the small model, which is more slimmer by using the starting dimension 64 instead of 96.

Comparison with PVT. PVT utilizes totally global attentions as DeiT while our method makes use of spatial separable-like design: locally-grouped attention and global sub-sampled attention.

Comparison with Swin. Swin utilizes the alternation of local window based attention and shifted window. The shifted window is used to communicate with different patches and increases the receptive field. Therefore, the receptive field increases with the depth of network. Moreover, they carefully design cyclic-shifting for efficient inference and utilize relative positional embeddings. This procedure is complicated and may not be optimized for speed on devices such as mobile devices. Our approach is much simpler and friendly to existing frameworks because it is built on commonly supported operations. Moreover, our local-global design can better exploit the global context, which is known to play an important role in many vision tasks.

4 Experiments

We report experiment results to verify the effectiveness of our models.

Algorithm 1 PyTorch snippet of locally grouped attention.

```

class GroupAttention(nn.Module):
    def __init__(self, dim, num_heads=8, qkv_bias=False, qk_scale=None, attn_drop=0., proj_drop=0., k1
                 =7, k2=7):
        super(GroupAttention, self).__init__()
        self.dim = dim
        self.num_heads = num_heads
        head_dim = dim // num_heads
        self.scale = qk_scale or head_dim ** -0.5
        self.qkv = nn.Linear(dim, dim * 3, bias=qkv_bias)
        self.attn_drop = nn.Dropout(attn_drop)
        self.proj = nn.Linear(dim, dim)
        self.proj_drop = nn.Dropout(proj_drop)
        self.k1 = k1
        self.k2 = k2
    def forward(self, x, H, W):
        B, N, C = x.shape
        h_group, w_group = H // self.k1, W // self.k2
        total_groups = h_group * w_group
        x = x.reshape(B, h_group, self.k1, w_group, self.k2, C).permute(0, 3, 1, 2, 4, 5)
        qkv = self.qkv(x).reshape(B, total_groups, -1, 3, self.num_heads, C // self.num_heads).
            permute(3, 0, 1, 4, 2, 5)
        q, k, v = qkv[0], qkv[1], qkv[2]
        attn = (q @ k.transpose(-2, -1)) * self.scale
        attn = attn.softmax(dim=-1)
        attn = self.attn_drop(attn)
        attn = (attn @ v).transpose(2, 3).reshape(B, h_group, w_group, self.k1, self.k2, C)
        x = attn.transpose(2, 3).reshape(B, N, C)
        x = self.proj(x)
        x = self.proj_drop(x)
    return x

```

Table 2 – Configuration details of Twins-SVT.

	Output Size	Layer Name	Twins-SVT-S	Twins-SVT-B	Twins-SVT-L
Stage 1	$\frac{H}{4} \times \frac{W}{4}$	Patch Embedding	$P_1 = 4; C_1 = 64$	$P_1 = 4; C_1 = 96$	$P_1 = 4; C_1 = 128$
		Transformer	LSA	LSA	LSA
		Encoder w/ PEG	GSA	GSA	GSA
Stage 2	$\frac{H}{8} \times \frac{W}{8}$	Patch Embedding	$P_2 = 2; C_2 = 128$	$P_2 = 2; C_2 = 192$	$P_2 = 2; C_2 = 256$
		Transformer	LSA	LSA	LSA
		Encoder w/ PEG	GSA	GSA	GSA
Stage 3	$\frac{H}{16} \times \frac{W}{16}$	Patch Embedding	$P_3 = 2; C_3 = 256$	$P_3 = 2; C_3 = 384$	$P_3 = 2; C_3 = 512$
		Transformer	LSA	LSA	LSA
		Encoder w/ PEG	GSA	GSA	GSA
Stage 4	$\frac{H}{32} \times \frac{W}{32}$	Patch Embedding	$P_4 = 2; C_4 = 512$	$P_4 = 2; C_4 = 768$	$P_4 = 2; C_4 = 1024$
		Transformer	$[GSA] \times 4$	$[GSA] \times 2$	$[GSA] \times 2$
		Encoder w/ PEG			

4.1 Classification on ImageNet

We carefully control the experiment settings to make fair comparisons against recent works [2, 8, 9]. All our models are trained for 300 epochs with a batch size of 1024 using the AdamW optimizer [41]. The learning rate is initialized to be 0.001 and decayed to zero within 300 epochs following the cosine strategy. We use a linear warm-up in the first five epochs and the same regularization setting as in [2]. Note that we do not utilize extra tricks in [32, 34] to make fair comparisons although it may further improve the performance of our method. We use increasing stochastic depth [42] augmentation of 0.2, 0.3, 0.5 for small, base and large model respectively. We use gradient clipping with a max norm of 5.0 to stabilize the training process, which is especially important for the training of our large models.

We report the classification results on ImageNet in Table 3. Twins-PCPVT-S outperforms PVT-small by 1.4% and obtains similar result as Swin-T with 18% fewer FLOPs. Twins-SVT-S is comparable to Swin-T with about 35% fewer FLOPs. Other models demonstrate similar advantages.

It is interesting to see that, without bells and whistles, Twins-PCPVT performs *on par* with the recent state-of-the-art Swin, which is based on much more sophisticated designs as mentioned above.

Table 3 – Comparisons with state-of-the-art methods for ImageNet classification. Throughput is tested on the batch size of 192. All models are trained and evaluated on 224×224 resolution. † : w/ CPVT’s position encodings [9].

Method	Param (M)	FLOPs (G)	Throughput (Images/s)	Top-1 (%)
ConvNet				
RegNetY-4G [43]	21	4.0	1157	80.0
RegNetY-8G [43]	39	8.0	592	81.7
RegNetY-16G [43]	84	16.0	335	82.9
Transformer				
DeiT-Small/16 [2]	22.1	4.6	437	79.9
CrossViT-S [36]	26.7	5.6	-	81.0
T2T-ViT-14 [33]	22	5.2	-	81.5
TNT-S [21]	23.8	5.2	-	81.3
CoaT Mini [23]	10	6.8	-	80.8
CoaT-Lite Small [23]	20	4.0	-	81.9
PVT-Small [8]	24.5	3.8	820	79.8
CPVT-Small-GAP [9]	23	4.6	817	81.5
Twins-PCPVT-S (ours)	24.1	3.7	815	81.2 (+1.3)
Swin-T [4]	29	4.5	766	81.3
Swin-T + CPVT †	28	4.4	766	81.2
Twins-SVT-S (ours)	24	2.8	1059	81.3 (+1.4)
T2T-ViT-19 [33]	39.2	8.9	-	81.9
PVT-Medium [8]	44.2	6.7	526	81.2
Twins-PCPVT-B(ours)	43.8	6.4	525	82.7 (+0.8)
Swin-S [4]	50	8.7	444	83.0
Twins-SVT-B (ours)	56.0	8.3	469	83.1 (+1.2)
ViT-Base/16 [1]	86.6	17.6	86	77.9
DeiT-Base/16 [2]	86.6	17.6	292	81.8
T2T-ViT-24 [33]	64.1	14.1	-	82.3
CrossViT-B [36]	104.7	21.2	-	82.2
TNT-B [21]	66	14.1	-	82.8
CPVT-B [9]	88	17.6	292	82.3
PVT-Large [8]	61.4	9.8	367	81.7
Swin-B [4]	88	15.4	275	83.3
Twins-SVT-L (ours)	99.2	14.8	288	83.3 (+5.4)
Hybrid				
BoTNet-S1-59 [35]	33.5	7.3	-	81.7
BossNet-T1 [44]	-	7.9	-	81.9
CvT-13 [37]	20	4.5	-	81.6
BoTNet-S1-110 [35]	54.7	10.9	-	82.8
CvT-21 [37]	32	7.1	-	82.5

Moreover, Twins-SVT also achieves similar or slightly better results, compared to Swin, indicating that the spatial separable-like design is a effective and promising paradigm.

We also replace the relative position encoding of Swin-T with PEG [9] but the performance cannot be improved (81.2%).

4.2 Semantic Segmentation on ADE20K

We further evaluate the performance on segmentation tasks. We test on the ADE20K dataset [45], a challenging scene parsing task for semantic segmentation, which is popularly evaluated by recent transformer based methods. This dataset contains 20K images for training and 2K images for validation. Following the common practices, we use the training set to train our models and report the mIoU on the validation set. To make fair comparisons, we use the Semantic FPN framework [46] and exactly the same training settings as in PVT [8]. Specifically, we train 80K steps with a batch size of 16 using AdamW [41]. The learning rate is initialized as 1×10^{-4} and scheduled by the

‘poly’ strategy with the power coefficient of 0.9. We apply the drop-path regularization of 0.2 for the backbone and weight decay 0.0005 for the whole network. Note that we use a stronger drop-path regularization of 0.4 for the large model to avoid over-fitting. For Swin, we use their official code and trained models. We report the result in Table 4.

With comparable FLOPs, Twins-PCPVT-S outperforms PVT-Small with a large margin (4.5% mIoU), which also surpasses ResNet50 by 7.6% mIoU. It also outperforms Swin-T with a clear margin. Besides, Twins-PCPVT-B also achieves 3.3% higher mIoU over PVT-Medium. As for our Twins-SVT models, Twins-SVT-S achieves better performance (+1.1%) than Swin-T. Twins-SVT-B obtains comparable performance as that of Swin-B.

4.3 Object Detection and Segmentation on COCO

We evaluate the performance of our method using two representative frameworks: RetinaNet [47] and Mask RCNN [48]. Specifically, we use our transformer models to build the backbones of these detectors. All the models are trained under the same setting as in [8]. Since PVT and Swin report their results using different frameworks, we try to make fair comparison and build consistent settings for future methods. We report standard $1 \times$ -schedule (12 epochs) detection results on the COCO 2017 dataset [49] in Tables 5 and 6. As for the evaluation based on RetinaNet, we train all the models using AdamW [41] optimizer for 12 epochs with a batch size of 16. The initial learning rate is 1×10^{-4} , started with 500-

iteration warmup and decayed by $10 \times$ at the 8th and 11th epoch. We use stochastic drop path regularization of 0.2 and weight decay 0.0001. The implementation is based on MMDetection [50]. For the Mask R-CNN framework, we use the initial learning rate of 2×10^{-4} as in [8]. All other hyper-parameters follow the default settings in MMDetection.

For object detection with RetinaNet, Twins-PCPVT-S surpasses PVT-Small with 2.6% mAP and Twins-PCPVT-B exceeds PVT-Medium by 2.4% mAP on the COCO val2017 split. Twins-SVT-S outperforms Swin-T with 0.8% mAP while using 15% fewer FLOPs.

For object segmentation with the Mask R-CNN framework, Twins-PCPVT-S brings similar boosted performance (2.5% mAP) over PVT-Small. Compared with PVT-Medium, Twins-PCPVT-B obtains 2.6% higher mAP, which is also on par with that of Swin. Both Twins-SVT-S and Twins-SVT-B achieve better or slightly better performance compared to the corresponding counterpart of Swin.

4.4 Ablation Studies

Configuration of local and global blocks We evaluate different forms of local and global combination using our small model and present the ablation results in Table 7. The transformers with only locally-grouped attention fail to obtain good performance because this setting has limited and small receptive field. An extra global attention in the

Table 4 – Performance comparisons with different backbones on ADE20K validation dataset. FLOPs is tested on 1024×1024 .

Backbone	Semantic FPN 80k		
	FLOPs (G)	Param (M)	mIoU (%)
ResNet50 [12]	183	28.5	36.7
PVT-Small [8]	161	28.2	39.8
Swin-T [4]	182	31.9	41.5
Twins-PCPVT-S (ours)	162	28.4	44.3 (+7.6)
Twins-SVT-S (ours)	144	28.3	42.6 (+5.9)
ResNet101 [12]	260	47.5	38.8
PVT-Medium [8]	219	48.0	41.6
Swin-S [4]	274	53.2	45.2
Twins-PCPVT-B (ours)	220	48.1	44.9 (+6.1)
Twins-SVT-B (ours)	261	60.4	45.0 (+6.0)
ResNetXt101-64 \times 4d [15]	-	86.4	40.2
PVT-Large [8]	283	65.1	42.1
Twins-SVT-L (ours)	397	103.7	45.8 (+5.6)

Table 7 – Classification performance for different configuration of local (L) and global (G) blocks based on the small scale model.

Function Type	Params (M)	FLOPs (G)	Top-1 (%)
(L, L, L)	8.8	2.2	76.6
(L, LLG, LLG, G)	23.5	2.8	81.2
(L, LG, LG, G)	24.1	2.8	81.3
(L, L, L, G)	22.2	2.9	80.5
PVT-small (G, G, G, G) [8]	24.5	3.8	79.8

Table 5 – Object detection performance on the COCO val2017 split using the RetinaNet framework. FLOPs is evaluated on 1280×800 .

Backbone	FLOPs (G)	#Param (M)	RetinaNet 1×					
			AP	AP ₅₀	AP ₇₅	AP _S	AP _M	AP _L
ResNet50 [12]	234	37.7	36.3	55.3	38.6	19.3	40.0	48.8
PVT-Small [8]	226	34.2	40.4	61.3	43.0	25.0	42.9	55.7
Twins-PCPVT-S (ours)	226	34.4	43.0 (+6.7)	64.1	46.0	27.5	46.3	57.3
Swin-T [4]	245	38.5	41.5	62.1	44.2	25.1	44.9	55.5
Swin-T+CPVT	245	38.5	41.3	62.4	44.1	26.2	44.5	55.4
Twins-SVT-S (ours)	209	34.3	42.3 (+6.0)	63.4	45.2	26.0	45.5	56.5
ResNet101 [12]	315	56.7	38.5	57.8	41.2	21.4	42.6	51.1
ResNeXt101-32 \times 4d [15]	319	56.4	39.9	59.6	42.7	22.3	44.2	52.5
PVT-Medium [8]	283	53.9	41.9	63.1	44.3	25.0	44.9	57.6
Twins-PCPVT-B (ours)	283	54.1	44.3 (+5.8)	65.6	47.3	27.9	47.9	59.6
Swin-S [4]	335	59.8	44.5	65.7	47.5	27.4	48.0	59.9
Twins-SVT-B (ours)	322	67.0	44.4 (+5.9)	65.8	47.4	27.9	47.8	59.5
ResNeXt101-64 \times 4d [15]	473	95.5	41.0	60.9	44.0	23.9	45.2	54.0
PVT-Large [8]	345	71.1	42.6	63.7	45.4	25.8	46.0	58.4
Twins-SVT-L (ours)	455	110.9	44.8 (+3.8)	66.1	48.1	28.4	48.3	60.1

Table 6 – Object detection and instance segmentation performance on the COCO val2017 dataset using the Mask R-CNN framework. FLOPs is evaluated on 1280×800 .

Backbone	FLOPs (G)	Param (M)	Mask R-CNN 1×					
			AP ^b	AP ₅₀ ^b	AP ₇₅ ^b	AP ^m	AP ₅₀ ^m	AP ₇₅ ^m
ResNet50 [12]	260	44.2	38.0	58.6	41.4	34.4	55.1	36.7
PVT-Small [8]	245	44.1	40.4	62.9	43.8	37.8	60.1	40.3
Twins-PCPVT-S (ours)	245	44.3	42.9 (+4.9)	65.8	47.1	40.0 (+5.6)	62.7	42.9
Swin-T [4]	264	47.8	42.2	64.6	46.2	39.1	61.6	42.0
Swin-T+CPVT	263	47.8	42.0	64.5	45.9	39.1	61.6	42.0
Twins-SVT-S (ours)	228	44.0	42.7 (+4.7)	65.6	46.7	39.6 (+5.2)	62.5	42.6
ResNet101 [12]	336	63.2	40.4	61.1	44.2	36.4	57.7	38.8
ResNeXt101-32 \times 4d [15]	340	62.8	41.9	62.5	45.9	37.5	59.4	40.2
PVT-Medium [8]	302	63.9	42.0	64.4	45.6	39.0	61.6	42.1
Twins-PCPVT-B (ours)	302	64.0	44.6 (+4.2)	66.7	48.9	40.9 (+4.5)	63.8	44.2
Swin-S [4]	354	69.1	44.8	66.6	48.9	40.9	63.4	44.2
Twins-SVT-B (ours)	340	76.3	45.1 (+4.7)	67.0	49.4	41.1 (+4.7)	64.1	44.4
ResNeXt101-64 \times 4d [15]	493	101.9	42.8	63.8	47.3	38.4	60.6	41.3
PVT-Large [8]	364	81.0	42.9	65.0	46.6	39.5	61.9	42.5
Twins-SVT-L (ours)	474	119.7	45.2 (+2.4)	67.5	49.4	41.2 (+2.8)	64.5	44.5

last stage can improve the classification performance by 3.2%. Local-Local-Global (*abbr.* LLG) also achieves good performance, but we do not use this design because it is not flexible to be extended to other vision tasks.

Representative function We further study how the different sub-sampled functions affect the performance. Specifically, we compare the regular strided convolutions, separable convolutions and average pooling based on the ‘small’ model and present the results in Table 8. The first option performs best and therefore we choose it as our default implementation.

Table 8 – ImageNet classification performance of different forms of representative function for Twins-SVT-S.

Function Type	Top-1(%)
2D Conv.	81.2
2D Separable Conv.	80.8
Average Pooling	80.8

5 Conclusion

In this paper, we have presented two powerful vision transformer backbones for both image-level classification and a few downstream dense prediction tasks. We dub them as twin transformers: Twins-PCPVT and Twins-GVT. The former variant explores the applicability of conditional positional encodings [9] in pyramid vision transformer [8], confirming its potential for improving backbones in many vision tasks. In latter variant we revisit current attention design to proffer a more efficient attention paradigm. We find that interleaving local and global attention can produce impressive results, yet it comes with higher throughputs. *Both transformer models set a new state of the art in image classification, objection detection and semantic/instance segmentation.*

References

- [1] Alexey Dosovitskiy, Lucas Beyer, Alexander Kolesnikov, Dirk Weissenborn, Xiaohua Zhai, Thomas Unterthiner, Mostafa Dehghani, Matthias Minderer, Georg Heigold, Sylvain Gelly, Jakob Uszkoreit, and Neil Houlsby. An image is worth 16x16 words: Transformers for image recognition at scale. In *International Conference on Learning Representations*, 2021.
- [2] Hugo Touvron, Matthieu Cord, Matthijs Douze, Francisco Massa, Alexandre Sablayrolles, and Hervé Jégou. Training data-efficient image transformers & distillation through attention. *arXiv preprint arXiv:2012.12877*, 2020.
- [3] Nicolas Carion, Francisco Massa, Gabriel Synnaeve, Nicolas Usunier, Alexander Kirillov, and Sergey Zagoruyko. End-to-end object detection with transformers. In *European Conference on Computer Vision*, pages 213–229. Springer, 2020.
- [4] Ze Liu, Yutong Lin, Yue Cao, Han Hu, Yixuan Wei, Zheng Zhang, Stephen Lin, and Baining Guo. Swin transformer: Hierarchical vision transformer using shifted windows. *arXiv preprint arXiv:2103.14030*, 2021.
- [5] Liang-Chieh Chen, George Papandreou, Iasonas Kokkinos, Kevin Murphy, and Alan L Yuille. Deeplab: Semantic image segmentation with deep convolutional nets, atrous convolution, and fully connected crfs. *IEEE transactions on pattern analysis and machine intelligence*, 40(4):834–848, 2017.
- [6] Chao Peng, Xiangyu Zhang, Gang Yu, Guiming Luo, and Jian Sun. Large kernel matters—improve semantic segmentation by global convolutional network. In *Proceedings of the IEEE conference on computer vision and pattern recognition*, pages 4353–4361, 2017.
- [7] Wei Liu, Andrew Rabinovich, and Alexander C Berg. Parsenet: Looking wider to see better. *arXiv preprint arXiv:1506.04579*, 2015.
- [8] Wenhui Wang, Enze Xie, Xiang Li, Deng-Ping Fan, Kaitao Song, Ding Liang, Tong Lu, Ping Luo, and Ling Shao. Pyramid vision transformer: A versatile backbone for dense prediction without convolutions. *arXiv preprint arXiv:2102.12122*, 2021.
- [9] Xiangxiang Chu, Zhi Tian, Bo Zhang, Xinlong Wang, Xiaolin Wei, Huaxia Xia, and Chunhua Shen. Conditional positional encodings for vision transformers. *arXiv preprint arXiv:2102.10882*, 2021.
- [10] Alex Krizhevsky, Ilya Sutskever, and Geoffrey E Hinton. Imagenet classification with deep convolutional neural networks. *Advances in neural information processing systems*, 25:1097–1105, 2012.
- [11] Christian Szegedy, Wei Liu, Yangqing Jia, Pierre Sermanet, Scott Reed, Dragomir Anguelov, Dumitru Erhan, Vincent Vanhoucke, and Andrew Rabinovich. Going deeper with convolutions. In *Proceedings of the IEEE conference on computer vision and pattern recognition*, pages 1–9, 2015.
- [12] Kaiming He, Xiangyu Zhang, Shaoqing Ren, and Jian Sun. Deep residual learning for image recognition. In *Proceedings of the IEEE conference on computer vision and pattern recognition*, pages 770–778, 2016.
- [13] Mingxing Tan and Quoc Le. Efficientnet: Rethinking model scaling for convolutional neural networks. In *International Conference on Machine Learning*, pages 6105–6114. PMLR, 2019.
- [14] François Chollet. Xception: Deep learning with depthwise separable convolutions. In *Proceedings of the IEEE conference on computer vision and pattern recognition*, pages 1251–1258, 2017.
- [15] Saining Xie, Ross Girshick, Piotr Dollár, Zhuowen Tu, and Kaiming He. Aggregated residual transformations for deep neural networks. In *Proceedings of the IEEE conference on computer vision and pattern recognition*, pages 1492–1500, 2017.

- [16] Andrew G Howard, Menglong Zhu, Bo Chen, Dmitry Kalenichenko, Weijun Wang, Tobias Weyand, Marco Andreetto, and Hartwig Adam. Mobilenets: Efficient convolutional neural networks for mobile vision applications. *arXiv preprint arXiv:1704.04861*, 2017.
- [17] Mark Sandler, Andrew Howard, Menglong Zhu, Andrey Zhmoginov, and Liang-Chieh Chen. Mobilenetv2: Inverted residuals and linear bottlenecks. In *Proceedings of the IEEE conference on computer vision and pattern recognition*, pages 4510–4520, 2018.
- [18] Jie Hu, Li Shen, and Gang Sun. Squeeze-and-excitation networks. In *Proceedings of the IEEE conference on computer vision and pattern recognition*, pages 7132–7141, 2018.
- [19] Xiangyu Zhang, Xinyu Zhou, Mengxiao Lin, and Jian Sun. Shufflenet: An extremely efficient convolutional neural network for mobile devices. In *Proceedings of the IEEE conference on computer vision and pattern recognition*, pages 6848–6856, 2018.
- [20] Ashish Vaswani, Noam Shazeer, Niki Parmar, Jakob Uszkoreit, Llion Jones, Aidan N Gomez, Łukasz Kaiser, and Illia Polosukhin. Attention is all you need. In *Proceedings of the 31st International Conference on Neural Information Processing Systems*, pages 6000–6010, 2017.
- [21] Kai Han, An Xiao, Enhua Wu, Jianyuan Guo, Chunjing Xu, and Yunhe Wang. Transformer in transformer. *arXiv preprint arXiv:2103.00112*, 2021.
- [22] Prajit Ramachandran, Niki Parmar, Ashish Vaswani, Irwan Bello, Anselm Levskaya, and Jon Shlens. Stand-alone self-attention in vision models. In H. Wallach, H. Larochelle, A. Beygelzimer, F. d’Alché-Buc, E. Fox, and R. Garnett, editors, *Advances in Neural Information Processing Systems*, volume 32, pages 68–80. Curran Associates, Inc., 2019.
- [23] Weijian Xu, Yifan Xu, Tyler Chang, and Zhuowen Tu. Co-scale conv-attentional image transformers, 2021.
- [24] Yuqing Wang, Zhaoliang Xu, Xinlong Wang, Chunhua Shen, Baoshan Cheng, Hao Shen, and Huaxia Xia. End-to-end video instance segmentation with transformers. In *Proc. IEEE Conf. Computer Vision and Pattern Recognition (CVPR)*, 2021.
- [25] Hanting Chen, Yunhe Wang, Tianyu Guo, Chang Xu, Yiping Deng, Zhenhua Liu, Siwei Ma, Chunjing Xu, Chao Xu, and Wen Gao. Pre-trained image processing transformer. *arXiv preprint arXiv:2012.00364*, 2020.
- [26] Fuzhi Yang, Huan Yang, Jianlong Fu, Hongtao Lu, and Baining Guo. Learning texture transformer network for image super-resolution. In *Proceedings of the IEEE/CVF Conference on Computer Vision and Pattern Recognition*, pages 5791–5800, 2020.
- [27] Yanhong Zeng, Jianlong Fu, and Hongyang Chao. Learning joint spatial-temporal transformations for video inpainting. In *European Conference on Computer Vision*, pages 528–543. Springer, 2020.
- [28] Zhigang Dai, Bolun Cai, Yugeng Lin, and Junying Chen. Up-detr: Unsupervised pre-training for object detection with transformers. *arXiv preprint arXiv:2011.09094*, 2020.
- [29] Aravind Srinivas, Tsung-Yi Lin, Niki Parmar, Jonathon Shlens, Pieter Abbeel, and Ashish Vaswani. Bottleneck transformers for visual recognition. 2021.
- [30] Sixiao Zheng, Jiachen Lu, Hengshuang Zhao, Xiatian Zhu, Zekun Luo, Yabiao Wang, Yanwei Fu, Jianfeng Feng, Tao Xiang, Philip HS Torr, et al. Rethinking semantic segmentation from a sequence-to-sequence perspective with transformers. *arXiv preprint arXiv:2012.15840*, 2020.
- [31] Niki Parmar, Ashish Vaswani, Jakob Uszkoreit, Łukasz Kaiser, Noam Shazeer, Alexander Ku, and Dustin Tran. Image transformer. In Jennifer Dy and Andreas Krause, editors, *Proceedings of the 35th International Conference on Machine Learning*, volume 80 of *Proceedings of Machine Learning Research*, pages 4055–4064, Stockholmsmässan, Stockholm Sweden, 10–15 Jul 2018. PMLR.
- [32] Hugo Touvron, Matthieu Cord, Alexandre Sablayrolles, Gabriel Synnaeve, and Hervé Jégou. Going deeper with image transformers. *arXiv preprint arXiv:2103.17239*, 2021.
- [33] Li Yuan, Yunpeng Chen, Tao Wang, Weihao Yu, Yujun Shi, Francis EH Tay, Jiashi Feng, and Shuicheng Yan. Tokens-to-token vit: Training vision transformers from scratch on imagenet. *arXiv preprint arXiv:2101.11986*, 2021.
- [34] Zihang Jiang, Qibin Hou, Li Yuan, Daquan Zhou, Xiaojie Jin, Anran Wang, and Jiashi Feng. Token labeling: Training an 85.4with 56m parameters on imagenet, 2021.
- [35] Aravind Srinivas, Tsung-Yi Lin, Niki Parmar, Jonathon Shlens, Pieter Abbeel, and Ashish Vaswani. Bottleneck transformers for visual recognition. *arXiv preprint arXiv:2101.11605*, 2021.
- [36] Chun-Fu Chen, Quanfu Fan, and Rameswar Panda. Crossvit: Cross-attention multi-scale vision transformer for image classification. *arXiv preprint arXiv:2103.14899*, 2021.
- [37] Haiping Wu, Bin Xiao, Noel Codella, Mengchen Liu, Xiyang Dai, Lu Yuan, and Lei Zhang. Cvt: Introducing convolutions to vision transformers, 2021.

- [38] Xizhou Zhu, Weijie Su, Lewei Lu, Bin Li, Xiaogang Wang, and Jifeng Dai. Deformable detr: Deformable transformers for end-to-end object detection. In *International Conference on Learning Representations*, 2021.
- [39] Tsung-Yi Lin, Piotr Dollár, Ross Girshick, Kaiming He, Bharath Hariharan, and Serge Belongie. Feature pyramid networks for object detection. In *Proceedings of the IEEE conference on computer vision and pattern recognition*, pages 2117–2125, 2017.
- [40] Laurent Sifre and Stéphane Mallat. Rigid-motion scattering for texture classification. *arXiv preprint arXiv:1403.1687*, 2014.
- [41] Ilya Loshchilov and Frank Hutter. Decoupled weight decay regularization. In *International Conference on Learning Representations*, 2019.
- [42] Gao Huang, Yu Sun, Zhuang Liu, Daniel Sedra, and Kilian Q Weinberger. Deep networks with stochastic depth. In *European conference on computer vision*, pages 646–661. Springer, 2016.
- [43] Ilija Radosavovic, Raj Prateek Kosaraju, Ross Girshick, Kaiming He, and Piotr Dollár. Designing network design spaces. In *Proceedings of the IEEE/CVF Conference on Computer Vision and Pattern Recognition*, pages 10428–10436, 2020.
- [44] Changlin Li, Tao Tang, Guangrun Wang, Jiefeng Peng, Bing Wang, Xiaodan Liang, and Xiaojun Chang. Bossnas: Exploring hybrid cnn-transformers with block-wisely self-supervised neural architecture search. *arXiv preprint arXiv:2103.12424*, 2021.
- [45] Bolei Zhou, Hang Zhao, Xavier Puig, Sanja Fidler, Adela Barriuso, and Antonio Torralba. Scene parsing through ade20k dataset. In *Proceedings of the IEEE conference on computer vision and pattern recognition*, pages 633–641, 2017.
- [46] Alexander Kirillov, Ross Girshick, Kaiming He, and Piotr Dollár. Panoptic feature pyramid networks. In *Proceedings of the IEEE/CVF Conference on Computer Vision and Pattern Recognition*, pages 6399–6408, 2019.
- [47] Tsung-Yi Lin, Priya Goyal, Ross Girshick, Kaiming He, and Piotr Dollár. Focal loss for dense object detection. In *Proceedings of the IEEE international conference on computer vision*, pages 2980–2988, 2017.
- [48] Kaiming He, Georgia Gkioxari, Piotr Dollár, and Ross Girshick. Mask r-cnn. In *Proceedings of the IEEE international conference on computer vision*, pages 2961–2969, 2017.
- [49] Tsung-Yi Lin, Michael Maire, Serge Belongie, James Hays, Pietro Perona, Deva Ramanan, Piotr Dollár, and C Lawrence Zitnick. Microsoft coco: Common objects in context. In *European conference on computer vision*, pages 740–755. Springer, 2014.
- [50] Kai Chen, Jiaqi Wang, Jiangmiao Pang, Yuhang Cao, Yu Xiong, Xiaoxiao Li, Shuyang Sun, Wansen Feng, Ziwei Liu, Jiarui Xu, Zheng Zhang, Dazhi Cheng, Chenchen Zhu, Tianheng Cheng, Qijie Zhao, Buyu Li, Xin Lu, Rui Zhu, Yue Wu, Jifeng Dai, Jingdong Wang, Jianping Shi, Wanli Ouyang, Chen Change Loy, and Dahua Lin. MMDetection: Open mmlab detection toolbox and benchmark. *arXiv preprint arXiv:1906.07155*, 2019.